Title:

Migration alters oscillatory dynamics and promotes survival in connected bacterial populations

Authors:

Shreyas Gokhale[†,1], Arolyn Conwill[†,1], Tanvi Ranjan[2] and Jeff Gore[1,*]

[1] Physics of Living Systems, Department of Physics, Massachusetts Institute of Technology, Cambridge, MA 02139.

[2] John A. Paulson School of Engineering and Applied Sciences, Harvard University, Cambridge, MA 02138.

* To whom correspondence should be addressed. Email: gore@mit.edu

[†] These authors contributed equally to this work.

Abstract:

Migration influences population dynamics on networks, thereby playing a vital role in scenarios ranging from species extinction to epidemic propagation. While low migration rates prevent local populations from becoming extinct, high migration rates enhance the risk of global extinction by synchronizing the dynamics of connected populations. Here, we investigate this trade-off using two mutualistic strains of *E. coli* that exhibit population oscillations when co-cultured. In experiments, as well as in simulations using a mechanistic model, we observe that high migration rates lead to in-phase synchronization whereas intermediate migration rates perturb the oscillations and change their period. Further, our simulations predict, and experiments show, that connected populations subjected to more challenging antibiotic concentrations have the highest probability of survival at intermediate migration rates. Finally, we identify altered population dynamics, rather than recolonization, as the primary cause of extended survival.

Main Text:

Spatially extended populations can be distributed heterogeneously, often in the form of a network of relatively dense population patches connected to each other by migration (1, 2). In macroecology, population networks are pervasive in a variety of social and ecological settings such as human settlements connected by transportation routes (3), oceanic islands connected by migration (4), and faraway plant populations connected by seed dispersal (5, 6). Migration patterns shape the population dynamics on these networks (7–9) and can have a profound impact on population stability and persistence (5, 10, 11).

One major focus of both theoretical work and field studies on connected populations has been conservation ecology, particularly in the context of endangered species (12). In general, disconnected networks or fragmented habitats are considered undesirable because isolated populations are susceptible to extinction due to demographic stochasticity or environmental fluctuations (13). In the presence of migration, individuals from neighboring populations can stabilize an endangered population (14). In addition, migration can counteract stochastic extinction of a local population by creating a metacommunity with a larger total population size (10). Furthermore, migrants can repopulate nearby patches that have gone extinct (13, 15). The concept that migration can prevent permanent population collapse has led to the construction of 'conservation corridors' that are intended to prevent local extinctions by facilitating movement between previously unconnected habitat patches (16).

However, excessive migration can lead to in-phase synchronization of population dynamics in connected habitat patches (12, 17–21). In harsh environmental conditions, synchronization can enhance the risk of global stochastic extinction during periods of collective decrease in population size (12), since patches effectively merge into one large population in the limit of strong coupling (22). Accordingly, a number of computational models predict that intermediate migration rates optimize species persistence time and extend metapopulation extinction time, mainly due to recolonization events following local extinction (23–26). Such recolonization-mediated enhancement in survival has been observed experimentally in metapopulations of plants (5), plants and predatory mites (27), fruit flies (10), and ciliate predator-prey systems (15, 28).

Apart from enabling recolonization, migration can also perturb population dynamics, potentially giving rise to another mechanism of enhanced survival. Populations exhibiting deterministic oscillations are ideally suited to studying migration-induced perturbations in population dynamics. In particular, time course data enables both quantification of perturbations and identification of extinction and recolonization events, making it possible to ascertain the relative importance of each of these survival mechanisms. While theoretical work on nonlinear maps (29) and on predator-prey systems (30) has linked perturbed within-patch population dynamics to enhanced survival, experimental validation is lacking owing largely to difficulties in obtaining high-quality time series data.

Here, we develop a bacterial model system composed of two connected oscillating populations to elucidate the impact of migration on population dynamics (Fig. 1A). Our approach is similar to previous studies (31–37) that have employed simple microbial populations in a laboratory setting to test ecological theories. Although it forgoes the complexity of natural population networks, our system is ideal for systematically exploring the relationship between survival and perturbed population dynamics because it allows us to precisely control the migration rate as well as environmental conditions. We also use a mathematical model of antibiotic degradation by bacteria to better understand the effects of migration between patches on our experimental system.

In this work, we first quantify the onset of in-phase synchronization in benign environmental conditions, in which individual populations exhibit stable oscillations over the duration of the experiment (Fig. 1B). More importantly, we show that en route to synchronization, the system goes through a series of qualitatively distinct oscillatory dynamics that are not observed in the absence of migration. We further show that these new dynamics enable populations to endure longer in harsh environments, as evidenced by the increase in survival times for moderate levels of migration. We emphasize that intermediate migration rates can lead to different ecological outcomes, even though the migration rate is below the level necessary for the onset of synchronization (Fig. 1B). In a broader context, our results on two connected bacterial populations can be viewed as the first step in a bottom up approach aimed at probing the role of migration in the population dynamics of more complex networks.

Results:

In order to quantify effects such as synchronization in an experimental model system, we use a bacterial cross-protection mutualism that exhibits robust oscillatory population dynamics (31). The system is comprised of two strains of *Escherichia coli* that protect each other from antibiotics in the environment by producing resistance enzymes. One strain (AmpR) is resistant to the antibiotic ampicillin, and the other strain (ChlR) is resistant to the antibiotic chloramphenicol (Fig. 2A). Previous work has already demonstrated that a co-culture of AmpR and ChlR exhibits robust limit cycle oscillations as a function of time over a broad range of antibiotic concentrations, when subjected to serial daily dilutions into fresh media and antibiotics (31).

In the serial daily dilution scheme employed in our experiments (Fig. 2B), we propagated co-cultures of the AmpR and ChlR strains in ~24 hour growth-dilution cycles in 96-well plates under well-mixed conditions in the presence of LB media, ampicillin, and chloramphenicol. At the end of each growth cycle, we measured the total population density using spectrophotometry and the relative proportion of AmpR and ChlR cells using flow cytometry (see Materials and Methods). Next, we diluted the co-cultures by a factor of 100 into fresh media containing antibiotics and subjected them to another growth cycle for ~24 hours. Upon repeating these daily growth-dilution cycles for 15 days, we observed that the population density of AmpR (purple) as well as ChlR (green) cells oscillates with a period of 3 days (Fig. 2C, left panel). We note that the ratio of AmpR cells to ChlR cells constitutes an appropriate characterization of the state of the population because it also exhibits period-3 oscillations, with the oscillation amplitude spanning four orders of magnitude (Fig. 2C, right panel).

In order to examine the effects of migration, we studied pairs of co-cultures and coupled them via transfer of cells between the two patches of each pair. Fig. 3A depicts the growth-migration-dilution scheme employed in our experiments. The scheme is similar to the growth-dilution scheme discussed earlier (Fig. 2B), with two important additions. First, we consider two co-cultures instead of one, which we label as ‘habitat patches’ A and B. The second crucial addition is the migration step, which occurs after growing the co-cultures for 24 hours and measuring the total population density and relative abundances of the strains, but before dilution into fresh media.

In this step, we transfer a fraction m of the cells from each co-culture into the other (corresponding to a fixed volume). The mixed co-cultures are then diluted into fresh media with antibiotics and grown again for 24 hours, as done previously for individual co-cultures. This migration scheme allows us to vary the migration rate over several orders of magnitude, enabling us to experimentally probe the effect of migration on population dynamics, in a systematic manner.

Since migration is known to lead to in-phase synchronization in a variety of systems (12, 18–21), we first quantified the minimum migration rate necessary for the onset of synchronization under benign environmental conditions (10 μg/ml ampicillin, 8 μg/ml chloramphenicol), in which the system exhibits stable oscillations (Fig. 2C). For each migration rate, we performed daily growth-migration-dilution experiments with three initial relative abundances of AmpR to ChlR cells for each of two biological replicates, i.e. a total of six replicate pairs of co-cultures. While in-phase synchronization can sometimes be observed even at very low migration rates (and even at $m = 0$ when the two populations happen to oscillate in phase without coupling), all replicates showed in-phase synchronization for $m \geq 0.2$ (Fig. 3B). This strongly suggests that the onset of complete in-phase synchronization lies in the region $0.1 < m \leq 0.2$.

While synchronization is certainly an important effect, it is not clear whether it is the only effect that migration has on population dynamics. In particular, it is worth investigating whether there are additional qualitative differences in population oscillations at intermediate migration rates. To this end, we took a closer look at the population time series data as a function of increasing migration rate. It is evident that our coupled co-cultures exhibit period 3 oscillations in the absence of migration ($m = 0$, Fig. 3C) as well as very high migration rates ($m = 0.2$, Fig. 3E), the difference being that the oscillations are unsynchronized in the former case and in-phase synchronized in the latter. However, the period-3 oscillations are perturbed at intermediate migration rates, and we see signatures of other periods, such as period-4 oscillations at $m = 0.1$ (Fig. 3D). The perturbed oscillations may also reflect the presence of long transients (38). Interestingly, perturbed oscillations appear to be quite common for $m = 0.04$ and $m = 0.1$ but are not observed at very low or very high migration rates (Fig. S1).

The data in Fig. 3C-E demonstrate that migration not only synchronizes population dynamics but also alters them in a qualitative manner. To better understand the sequence of experimental outcomes with increasing migration rate, we turned to an ordinary differential equation based mechanistic model that simulates antibiotic degradation and cell growth. This model was developed in the context of isolated co-cultures and has been shown to reproduce the observed period-3 limit cycle oscillations over a reasonably broad parameter regime (31). The model has two variables N_1 and N_2 corresponding to the population densities of AmpR and ChlR, respectively, and two variables A_1 and A_2 corresponding to the concentrations of the antibiotics ampicillin and chloramphenicol, respectively. Over the 24 hour growth period, the population densities and antibiotic concentrations change with time according to the following equations:

$$\frac{dN_1}{dt} = \gamma_1(A_2)N_1\left(1 - \frac{N_1 + N_2}{K}\right)$$

$$\frac{dN_2}{dt} = \gamma_2(A_1)N_2\left(1 - \frac{N_1 + N_2}{K}\right)$$

$$\frac{dA_1}{dt} = \frac{-V_{max}A_1}{K_m + A_1}N_1(t = 0)$$

$$\frac{dA_2}{dt} = -c_2A_2N_2$$

Here, we assume that bacterial growth is logistic, with antibiotic concentration-dependent growth rates $\gamma_1(A_2)$ and $\gamma_2(A_1)$. The two strains exhibit neutral resource competition, as reflected in the combined carrying capacity K. Ampicillin degradation is assumed to obey Michaelis-Menten kinetics. In reality, ampicillin is degraded by β-lactamase (39, 40) molecules produced by AmpR cells during their growth as well as the free ones carried over from the previous day. Our model assumes that the dominant contribution comes from the β-lactamases carried over from the previous day. Since the number of enzyme molecules carried over is proportional to the number of AmpR cells present at the beginning of the day, the equation for A_1contains the initial density of AmpR cells $N_1(t = 0)$ rather than their instantaneous density $N_1(t)$. Since chloramphenicol degradation is intracellular (39), the degradation rate of chloramphenicol is taken to be proportional to the density of ChlR cells. Finally, since AmpR cells are sensitive to chloramphenicol, and ChlR cells are sensitive to ampicillin, the growth rates of the two strains are

proportional to the concentration of the antibiotic to which they are sensitive. These growth rates are given by:

$$\gamma_1(A_2) = \begin{cases} 0 & t < t_{lag} \\ \dfrac{\gamma_1^R}{1 + A_2/I_{12}} & t \geq t_{lag} \end{cases}$$

$$\gamma_2(A_1) = \begin{cases} 0 & t < t_{lag} \\ -\gamma_2^D + \dfrac{\gamma_2^R + \gamma_2^D}{1 + A_1/I_{21}} & t \geq t_{lag} \end{cases}$$

Here, we have also incorporated a lag phase, characterized by a time scale t_{lag} over which the cells do not grow or die. Since chloramphenicol is a bacteriostatic antibiotic, i.e. it inhibits sensitive cell growth but does not cause the cells to die, the growth rate of AmpR cells approaches zero at high concentrations of chloramphenicol but never becomes negative (Fig. 4A, green curve). On the other hand, since ampicillin is a bactericidal antibiotic, i.e. its presence can cause sensitive cells to die, the growth rate of ChlR cells becomes negative at high concentrations of ampicillin (Fig. 4A, purple curve). Numerical values and descriptions of all parameters used in the simulations are listed in Table S1. In a typical simulation over a 24 hour growth cycle, the cell densities saturate (Fig. 4B, top panel) and the antibiotics are inactivated (Fig. 4B, bottom panel). We note that the initial and final densities of AmpR and ChR can be substantially different, such that the ratio N_1/N_2 can vary substantially from day to day.

To gain insight into the experimentally observed changes in oscillatory dynamics with increasing migration rate, we implemented the growth-migration-dilution scheme in our simulations. The chief advantage of simulations is that they allow us to analyze the system's behavior over timescales that are much longer than those accessible in our experiments. The long timescales enable us to discern whether a given dynamical outcome corresponds to stable oscillations or transient dynamics. Simulations also facilitate a detailed characterization of oscillatory dynamics as well as the range of migration rates over which they are observed. In our simulations, we started with two patches A and B for which we numerically integrated the model equations over 24 hours. To implement the migration and dilution steps, we mimicked the experimental protocol by

resetting the initial population densities and antibiotic concentrations in the two patches for the next day of growth in accordance with the dilution factor of 100 and the migration rate m. The system's dynamical outcomes are best summarized in the form of a bifurcation diagram as a function of the migration rate (Fig. 4C). In this bifurcation diagram we have plotted the unique values attained by the population, i.e. the ratio of AmpR to ChlR cells in patch A over the last 50 days of a simulation consisting of 1000 daily dilution cycles.

As expected, we observe a regime of period-3 oscillations at very low migration rates (Fig. 4C, blue region) as well as high migration rates (Fig. 4C, red region). Moreover, these oscillations are unsynchronized at very low migration rates and synchronized in-phase at high migration rates (Fig. 4C, insets corresponding to blue and red regions; also see Fig. S2 for the probability of in-phase synchronization as a function of the migration rate). Quite remarkably, the bifurcation diagram also contains a regime of period-4 limit cycle oscillations (Fig. 4C, orange region and inset) at intermediate migration rates that is surrounded on both sides by narrow regions characterized by irregular dynamics and long transients (Fig. 4C, green regions). The dynamics in these regions are strikingly similar to the perturbed oscillations observed in our experiments (Fig. 3D and Fig. S1). Indeed, our simple model successfully captures the sequence of experimentally observed dynamical outcomes as a function of the migration rate. In particular, transitions between different dynamical regimes are in reasonable qualitative agreement with our experiments. Moreover, the presence of altered population dynamics in both experiments and simulations suggests that intermediate migration rates can indeed give rise to population dynamics that are distinct from those in the uncoupled and synchronized regimes.

It is plausible that the disturbance of oscillations at intermediate migration rates may influence a population's viability in harsh environments, although it is not *a priori* obvious whether this influence would be harmful or beneficial. As mentioned earlier, it has been suggested that synchronization can enhance the risk of global extinction in harsh environments (12, 18), which implies that high migration rates may have a deleterious impact on the probability of survival, but it is not clear if this effect is monotonic. To explore the effect of intermediate migration rates on survival probability, we simulated our model in harsh environmental conditions. For these simulations, a harsh environment corresponds to higher antibiotic concentrations (10 μg/ml

ampicillin, 16 μg/ml chloramphenicol), where the model predicts that isolated populations go extinct deterministically in the absence of migration. Furthermore, we introduce 15% noise in the migration and dilution steps of our simulations, to mimic the stochastic fluctuations resulting from our experimental protocol. To quantify the impact of migration on survival, we generated probability distributions $P(\tau)$ of population lifetimes, i.e. the durations τ for which the populations survived for various m (Fig. 5A). The distributions decay exponentially over a timescale that increases with migration rate for $m \lesssim 0.03$ and decrease with migration rate for $m \gtrsim 0.1$. Interestingly, within a narrow intermediate migration regime ($0.04 \lesssim m \lesssim 0.07$), the survival time distributions have longer tails, which suggests that intermediate migration rates can result in enhanced survival as compared with isolated populations or strongly coupled ones. Overall, the variation of $P(\tau)$ with m indicates that moderate levels of migration offer the best chance of survival in harsh conditions.

A more experimentally tractable measure of the effect of migration on survival in challenging environments is the fraction of populations that survive over a given period of time. Towards this end, we computed the probability of survival over 10 days. As expected from the variation in $P(\tau)$ with m (Fig. 5A), the survival probability over 10 days changes non-monotonically with the migration rate (Fig. 5B). This qualitative trend occurs regardless of the duration over which we compute survival probability (Fig. S3). Moreover, the peak in survival probability occurs in the regime where we observe approximately exponential decay in $P(\tau)$, once again suggesting that moderate levels of migration perturb population dynamics in a manner that favors extended survival.

Motivated by the simulation results, we proceeded to test whether the predicted non-monotonicity of survival probability with m is also observed in experiments. Accordingly, we performed growth-dilution-migration experiments with higher antibiotic concentrations (10 μg/ml ampicillin, 16 μg/ml chloramphenicol) and measured the fraction of populations that survived over 10 days. As predicted by the simulations, the survival probability indeed shows a peak at intermediate migration rates (Fig. 5C; see Fig. S4 for population density time series). Further, the location of the maximum shows reasonably good quantitative agreement with the simulations. Collectively,

these findings establish that moderate levels of migration promote population dynamics that extended survival in harsh environments.

Discussion:

Here, we have shown that two oscillating bacterial populations can synchronize when coupled sufficiently strongly via migration. Furthermore, we have demonstrated that it is possible for the migration rate itself to determine the period of oscillation. In particular, our experimental system exhibits limit cycle period-3 oscillations in the absence of migration. However, we observed disturbances in these dynamics in the presence of migration that were consistent with the period-4 oscillations predicted by the model at intermediate migration rates (Fig. 3D). This finding represents empirical evidence that the characteristics of population oscillations observed in natural microbial communities may not simply be a result of intrinsic inter- or intra-species interactions, but may also be a consequence of spatial structure and migration.

Since migration can perturb population dynamics, it also has the potential to influence the survival of a population in a challenging environment. For instance, we found that populations were most likely to survive the duration of the experiment at intermediate migration rates (Fig. 5). The presence of a maximum in survival probability at intermediate migration rates is potentially relevant in conservation biology and epidemiology in that controlling migration might lead to desired outcomes like population stability or disease eradication. Interestingly, the dynamics we observe within this intermediate migration rate regime resemble noisy out-of-phase period-2 oscillations (see Fig. S5 for bifurcation diagrams and a representative time series), and we see signatures of such oscillations in some of our surviving experimental populations as well (Fig. S6). Intuitively, out-of-phase synchronization could ensure that the populations in the two patches do not simultaneously become low, which averts the danger of global extinction. In previous computational studies (23, 29, 41, 42), such out-of-phase synchronization has been widely recognized as a potential mechanism for survival and our experiments provide direct evidence in support of these numerical findings.

In field ecology and metapopulation theory, re-colonization of habitat patches after local extinction events is thought to be a major contributor to extended survival in harsh environments (13), a claim

supported by recent experiments on protists (15). However, we observed relatively few instances of such re-colonization (Fig. S7), implying that re-colonization is not the major cause of extended survival in our system. Nevertheless, in a more spatially extended population with a larger number of possible habitats, it may be possible that re-colonization plays a more significant role in enabling populations to survive in challenging conditions.

Finally, we note that in challenging environments, evolutionary rescue can also lead to population recovery (43). In our system, evolutionary rescue may occur either via enhanced antibiotic tolerance through the evolution of lag time mutants (44) or via increased drug resistance in one of the strains. Indeed, we did observe a few cases in which ChlR cells developed a higher resistance to ampicillin, particularly at high migration rates in the harsh environment (10 μg/ml ampicillin, 16 μg/ml chloramphenicol) (Fig. S8). Interestingly, we found no evidence of such evolution in extremely harsh environments (10 μg/ml ampicillin, 20 μg/ml chloramphenicol), in which all populations became extinct within 7 days (Fig. S9). Collectively, these observations suggest that the optimal conditions for evolution of additional antibiotic resistance represent a tradeoff between selection pressure, which is primarily determined by the environment, and survival time, which can be influenced by the migration rate. In addition, the effective population size may also play a role in guiding the course of evolution in that stronger coupling may lead to a larger population size and thus more genetic diversity, but may also lead to reduced survival time.

In the present study, we found that moderate amounts of migration between two coupled bacterial populations can significantly perturb population oscillations and enhance survival in harsh environments (Fig. 3D-E). Given that a simple setup can have significant ecological consequences, it would be interesting to extend this approach to a larger number of connected populations. For example, in addition to the migration rate, the network topology can play an important role in governing synchronization (45, 46). The network topology also allows exotic forms of partial synchronization such as phase clusters and chimeras (47–49), whose relevance to ecological systems is hitherto unexplored. The effects of asymmetric migration rates, spatial expansion, and environmental conditions are also worthy of exploration (41, 50–52).

More generally, our experiments suggest that it is worthwhile to explore how concepts from macroecology and network theory apply to microbial systems. Despite extensive work in theoretical ecology and macroecology, relatively little attention has been dedicated to examining the implications of migration on microbial communities, which can exhibit rich population dynamics over spatially extended environments. Spatially fragmented yet dispersed microbial communities can be found in the ocean on organic particulate matter called marine snow (53), in the ground on soil grains, and on different human body sites, suggesting that the impact of migration on the ecology of these microbial ecosystems may have implications on topics ranging from the global carbon cycle (54) to human health. Given that that there are notable differences between microbes and larger organisms (ex. relatively large population sizes with fewer stochastic fluctuations), further work is necessary to translate findings from theoretical ecology and macroecology to microbial ecology.

Materials and Methods:

Strains: The strains used are identical to those in (31). Briefly, the chloramphenicol-resistant strain ChlR is an *E. coli* DH5α strain transformed with the pBbS5c-RFP plasmid (55) which encodes a gene for chloramphenicol acetyltransferase (type I) enzyme as well as a gene for monomeric red fluorescent protein (RFP). The plasmid pbBS5c-RFP was obtained from Jay Keasling (University of California, Berkeley, CA) via Addgene (plasmid 35284) (55). The ampicillin-resistant strain is an *E. coli* DH5α strain transformed with a plasmid encoding a gene for the β-lactamase enzyme (TEM-1) and a gene for enhanced yellow fluorescent protein (EYFP).

Experiments: Initial monocultures of our strains were grown for 24 h in culture tubes containing 5 ml LB supplemented with antibiotic for selection (50 μg/mL ampicillin and 25 μg/mL chloramphenicol for AmpR and ChlR, respectively) at 37°C and shaken at 250 rpm. The following day, 200 μL of co-cultures of the two strains were grown at varying initial population fractions in LB without antibiotics. For synchronization experiments, the initial ratios of AmpR cells to ChlR cells were chosen such that the probability for paired co-cultures to be in the same phase of oscillation in the absence of migration ($m = 0$) was low. Subsequently, serial migration-dilution experiments were performed in well-mixed batch culture with a culture volume of 200 μL. In each cycle, co-cultures were grown for 24 hours in LB media supplemented with the antibiotics

ampicillin and chloramphenicol. During growth, cultures were shaken at 500 rpm at a temperature of 37°C. At the end of the growth cycle, we measured the optical density (OD) at 600 nm and prepared flow cytometry samples by diluting 5μL of each grown co-culture by a factor of 1600 into phosphate buffer (PBS, Corning 21-040-CV). To perform the migration step, we pipetted fixed volumes of each co-culture within a connected pair into the other at the end of each growth cycle; subsequently, these co-cultures were diluted by a factor of 100 into fresh LB media and antibiotics. Growth medium was prepared by using BD's Difco TM LB Broth (Miller) (catalog no. 244620). Ampicillin stock was prepared by dissolving ampicillin sodium salt (Sigma-Aldrich catalog no. A9518) in LB at a concentration of 50 mg/mL. The solution was filter sterilized, stored frozen at −20°C, and thawed before use. Chloramphenicol stock was prepared by dissolving chloramphenicol powder (Sigma-Aldrich catalog no. C0378) in 200 proof pure ethanol (KOPTEC) at a concentration of 25 mg/mL. This solution was filter sterilized and stored at −20°C. Prepared 96-well plates of media supplemented with antibiotics were stored at −80°C, thawed 1 d prior to inoculation at 4°C and warmed for 1hour at 37°C immediately before inoculation.

Measurement and Data Analysis: At the end of each growth cycle, we took spectrophotometric (Thermo Scientific Varioskan Flash at 600 nm) measurements, which serve as a proxy for the total population size. We converted the OD measurement to CFU/μl based on a calibration curve obtained from counting colonies on LB and agar plates originating from cultures at various cell densities. We also took flow cytometry (Miltenyi Biotec MACSQuant VYB) measurements of the cultures to determine subpopulation sizes. We consider two populations to be synchronized in-phase if the peaks of their oscillation occur at the same time over the last two oscillation cycles (the final 40% of the experiment), to reduce the influence of transients as well as gather sufficient statistics. Data analysis was performed using a combination of Matlab and Origin. Simulations were performed using Matlab. Flow cytometry data were analyzed using the Python package FlowCytometryTools (56). Data are available upon request.

Acknowledgements:

This work was primarily supported by NIH Grant R01 GM102311-01 and National Science Foundation CAREER Award PHY-1055154. The laboratory acknowledges support from the Pew Scholars in the Biomedical Sciences Program Grant 2010-000224-007, NIH R00 Pathways to

Independence Award GM085279-02, Sloan Foundation Fellowship BR2011-066, the Allen Distinguished Investigator Program, and NIH New Innovator Award DP2. S.G. was supported by a Human Frontier Science Program cross-disciplinary postdoctoral fellowship. We also thank members of the Gore Lab for helpful discussions.

Contributions:

A.C. and J.G. designed the research; S.G. and T.R. performed the research; S.G. and A.C. developed models; S.G. and A.C. analyzed data; and S.G., A.C., and J.G. wrote the paper.

Competing interests:

The authors declare no competing interests.

References:

1. Gilpin M (2012) *Metapopulation dynamics: empirical and theoretical investigations* (Academic Press).

2. Hanski I (1998) Metapopulation dynamics. *Nature* 396(6706):41.

3. Guimera R, Mossa S, Turtschi A, Amaral LN (2005) The worldwide air transportation network: Anomalous centrality, community structure, and cities' global roles. *Proc Natl Acad Sci* 102(22):7794–7799.

4. Cowie RH, Holland BS (2006) Dispersal is fundamental to biogeography and the evolution of biodiversity on oceanic islands. *J Biogeogr* 33(2):193–198.

5. Molofsky J, Ferdy J-B (2005) Extinction dynamics in experimental metapopulations. *Proc Natl Acad Sci U S A* 102(10):3726–3731.

6. Nathan R (2006) Long-distance dispersal of plants. *Science* 313(5788):786–788.

7. Blasius B, Huppert A, Stone L (1999) Complex dynamics and phase synchronization in spatially extended ecological systems. *Nature* 399(6734):354.

8. Limdi A, Perez-Escudero A, Li A, Gore J (2017) Asymmetric migration decreases stability but increases resilience in a heterogeneous metacommunity. *bioRxiv*. doi:10.1101/201723.

9. Gilarranz LJ, Rayfield B, Liñán-Cembrano G, Bascompte J, Gonzalez A (2017) Effects of network modularity on the spread of perturbation impact in experimental metapopulations. *Science* 357(6347):199–201.

10. Dey S, Joshi A (2006) Stability via asynchrony in Drosophila metapopulations with low migration rates. *Science* 312(5772):434–436.

11. Abbott KC (2011) A dispersal-induced paradox: synchrony and stability in stochastic metapopulations. *Ecol Lett* 14(11):1158–1169.

12. Earn DJ, Levin SA, Rohani P (2000) Coherence and conservation. *Science* 290(5495):1360–1364.

13. Harrison S (1991) Local extinction in a metapopulation context: an empirical evaluation. *Biol J Linn Soc* 42(1–2):73–88.

14. Gonzalez A, Lawton JH, Gilbert FS, Blackburn TM, Evans-Freke I (1998) Metapopulation dynamics, abundance, and distribution in a microecosystem. *Science* 281(5385):2045–2047.

15. Fox JW, Vasseur D, Cotroneo M, Guan L, Simon F (2017) Population extinctions can increase metapopulation persistence. *Nat Ecol Evol* 1(9):1271.

16. Hilty JA, Lidicker Jr WZ, Merenlender A (2012) *Corridor ecology: the science and practice of linking landscapes for biodiversity conservation* (Island Press).

17. Liebhold A, Koenig WD, Bjørnstad ON (2004) Spatial synchrony in population dynamics. *Annu Rev Ecol Evol Syst* 35:467–490.

18. Kerr B, Neuhauser C, Bohannan BJ, Dean AM (2006) Local migration promotes competitive restraint in a host-pathogen 'tragedy of the commons'. *Nature* 442(7098):75.

19. Grassly NC, Fraser C, Garnett GP (2005) Host immunity and synchronized epidemics of syphilis across the United States. *Nature* 433(7024):417.

20. Viboud C, et al. (2006) Synchrony, waves, and spatial hierarchies in the spread of influenza. *Science* 312(5772):447–451.

21. Grenfell BT, Bjørnstad ON, Kappey J (2001) Travelling waves and spatial hierarchies in measles epidemics. *Nature* 414(6865):716–723.

22. Ray C, Hastings A (1996) Density dependence: are we searching at the wrong spatial scale? *J Anim Ecol*:556–566.

23. Ben-Zion Y, Fried Y, Shnerb NM (2012) Migration, coherence and persistence in a fragmented landscape. *Theor Ecol* 5(4):481–493.

24. Yaari Gur, Ben-Zion Yossi, Shnerb Nadav M., Vasseur David A. (2012) Consistent scaling of persistence time in metapopulations. *Ecology* 93(5):1214–1227.

452 25. Khasin M, Meerson B, Khain E, Sander LM (2012) Minimizing the Population Extinction Risk by
453 Migration. *Phys Rev Lett* 109(13):138104.

454 26. Lampert A, Hastings A (2013) Synchronization-induced persistence versus selection for habitats
455 in spatially coupled ecosystems. *J R Soc Interface* 10(87). doi:10.1098/rsif.2013.0559.

456 27. Ellner SP, et al. (2001) Habitat structure and population persistence in an experimental
457 community. *Nature* 412:538.

458 28. Holyoak Marcel, Lawler Sharon P. (1996) Persistence of an Extinction-Prone Predator-Prey
459 Interaction Through Metapopulation Dynamics. *Ecology* 77(6):1867–1879.

460 29. Zion YB, Yaari G, Shnerb NM (2010) Optimizing metapopulation sustainability through a
461 checkerboard strategy. *PLoS Comput Biol* 6(1):e1000643.

462 30. Lampert Adam, Hastings Alan, Drake John (2016) Stability and distribution of predator–prey
463 systems: local and regional mechanisms and patterns. *Ecol Lett* 19(3):279–288.

464 31. Yurtsev EA, Conwill A, Gore J (2016) Oscillatory dynamics in a bacterial cross-protection
465 mutualism. *Proc Natl Acad Sci* 113(22):6236–6241.

466 32. Hoek TA, et al. (2016) Resource Availability Modulates the Cooperative and Competitive Nature
467 of a Microbial Cross-Feeding Mutualism. *PLOS Biol* 14(8):e1002540.

468 33. Müller MJI, Neugeboren BI, Nelson DR, Murray AW (2014) Genetic drift opposes mutualism
469 during spatial population expansion. *Proc Natl Acad Sci* 111(3):1037.

470 34. Fussmann GF, Ellner SP, Shertzer KW, Hairston Jr. NG (2000) Crossing the Hopf Bifurcation in a
471 Live Predator-Prey System. *Science* 290(5495):1358.

472 35. Becks Lutz, Ellner Stephen P., Jones Laura E., Hairston Jr Nelson G. (2010) Reduction of adaptive
473 genetic diversity radically alters eco-evolutionary community dynamics. *Ecol Lett* 13(8):989–997.

474 36. Zomorrodi AR, Segrè D (2016) Synthetic Ecology of Microbes: Mathematical Models and
475 Applications. *Eng Tools Prospects Synth Biol* 428(5, Part B):837–861.

476 37. Friedman J, Gore J (2017) Ecological systems biology: The dynamics of interacting populations.
477 *Future Syst Biol • Genomics Epigenomics* 1:114–121.

478 38. Wysham DB, Hastings A (2008) Sudden shifts in ecological systems: Intermittency and transients
479 in the coupled Ricker population model. *Bull Math Biol* 70(4):1013–1031.

480 39. Nicoloff H, Andersson DI (2015) Indirect resistance to several classes of antibiotics in cocultures
481 with resistant bacteria expressing antibiotic-modifying or-degrading enzymes. *J Antimicrob Chemother*
482 71(1):100–110.

40. Sykes RB, Matthew M (1976) The β-lactamases of gram-negative bacteria and their role in resistance to β-lactam antibiotics. *J Antimicrob Chemother* 2(2):115–157.

41. Dey S, Goswami B, Joshi A (2014) Effects of symmetric and asymmetric dispersal on the dynamics of heterogeneous metapopulations: two-patch systems revisited. *J Theor Biol* 345:52–60.

42. Dey S, Goswami B, Joshi A (2015) A possible mechanism for the attainment of out-of-phase periodic dynamics in two chaotic subpopulations coupled at low dispersal rate. *J Theor Biol* 367:100–110.

43. Bell G, Gonzalez A (2011) Adaptation and evolutionary rescue in metapopulations experiencing environmental deterioration. *Science* 332(6035):1327–1330.

44. Fridman O, Goldberg A, Ronin I, Shoresh N, Balaban NQ (2014) Optimization of lag time underlies antibiotic tolerance in evolved bacterial populations. *Nature* 513(7518):418.

45. Noble AE, Machta J, Hastings A (2015) Emergent long-range synchronization of oscillating ecological populations without external forcing described by Ising universality. *Nat Commun* 6.

46. Holland MD, Hastings A (2008) Strong effect of dispersal network structure on ecological dynamics. *Nature* 456(7223):792.

47. Abrams DM, Strogatz SH (2004) Chimera states for coupled oscillators. *Phys Rev Lett* 93(17):174102.

48. Tinsley MR, Nkomo S, Showalter K (2012) Chimera and phase-cluster states in populations of coupled chemical oscillators. *Nat Phys* 8(9):662.

49. Martens EA, Thutupalli S, Fourrière A, Hallatschek O (2013) Chimera states in mechanical oscillator networks. *Proc Natl Acad Sci* 110(26):10563–10567.

50. Franco D, Ruiz-Herrera A (2015) To connect or not to connect isolated patches. *J Theor Biol* 370:72–80.

51. Becks L, Arndt H (2013) Different types of synchrony in chaotic and cyclic communities. *Nat Commun* 4:1359.

52. Sullivan LL, Li B, Miller TE, Neubert MG, Shaw AK (2017) Density dependence in demography and dispersal generates fluctuating invasion speeds. *Proc Natl Acad Sci* 114(19):5053–5058.

53. Alldredge AL, Silver MW (1988) Characteristics, dynamics and significance of marine snow. *Prog Oceanogr* 20(1):41–82.

54. Azam F, Long RA (2001) Sea snow microcosms. *Nature* 414(6863):495–498.

55. Lee TS, et al. (2011) BglBrick vectors and datasheets: a synthetic biology platform for gene expression. *J Biol Eng* 5(1):12.

515 56. Yurtsev E, Friedman J, Gore J *FlowCytometryTools: Version 0.4.5*.

516

517

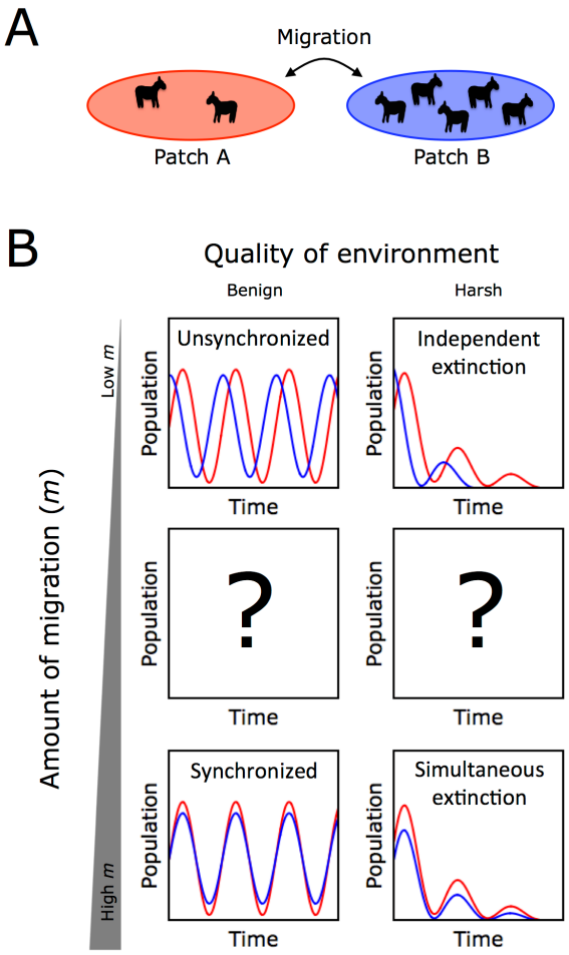

Fig 1: The cartoon illustrates possible qualitative effects of migration on population dynamics of a species in benign as well as harsh environmental conditions. A) The population dynamics of two patches can be coupled via migration. **B)** Under benign conditions, low migration rates are insufficient to couple population dynamics on the two patches (top left). On the other hand, high migration rates lead to in-phase synchronization, rendering the two patches equivalent (bottom left). An open question concerns how the population dynamics respond to intermediate migration rates (center left). In harsh conditions, population patches can become extinct (top right) and high migrations rate could lead to simultaneous extinction (bottom right). At intermediate migration rates, we investigate whether altered population dynamics could potentially lead to longer survival times (center right).

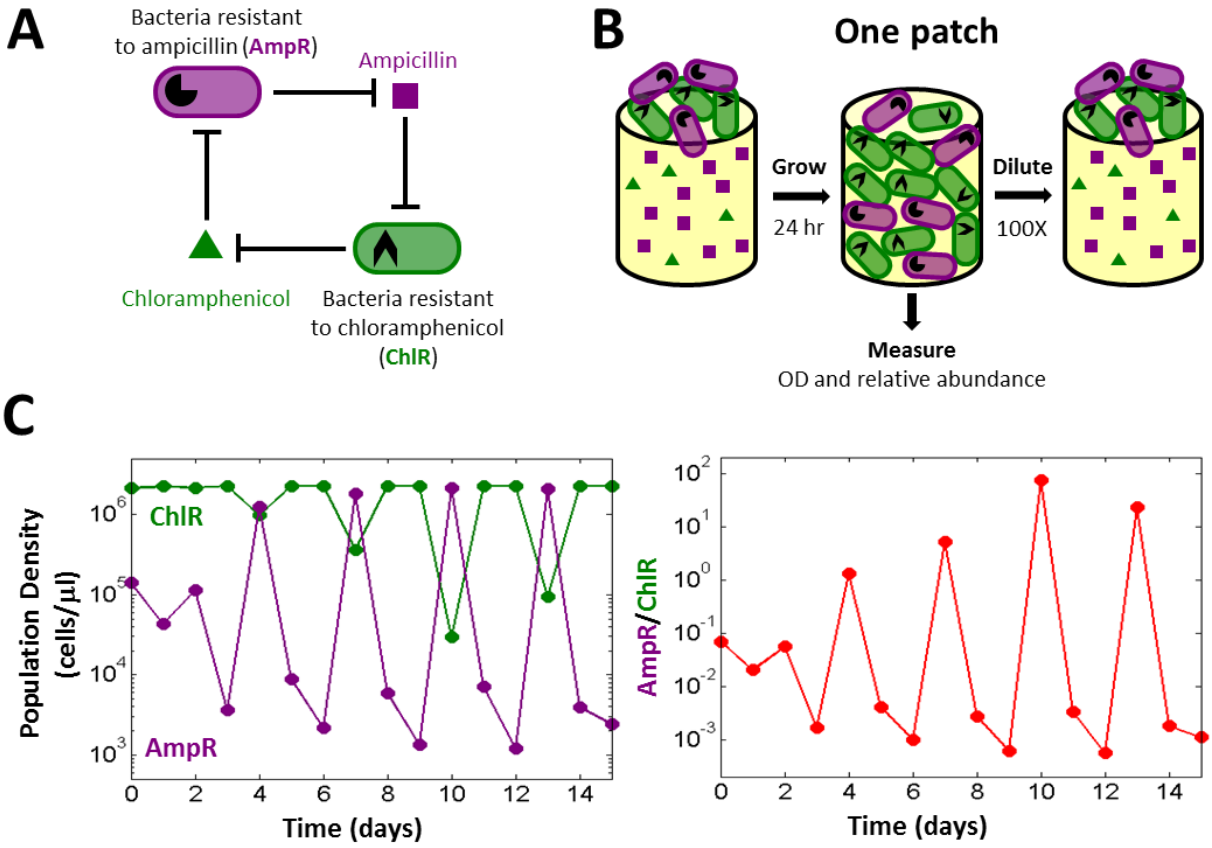

Fig 2: A bacterial cross-protection mutualism serves as a model system to study migration-induced synchronization of population oscillations. A) Diagram depicting the mutualistic interaction between ampicillin resistant (AmpR) and chloramphenicol resistant (ChlR) cells. AmpR cells protect ChlR cells by enzymatically deactivating ampicillin, whereas ChlR cells protect AmpR cells by deactivating chloramphenicol. **B)** Schematic illustration of the experimental growth-dilution scheme for growing isolated co-cultures in the absence of migration. Each day, cells are grown for 24 hours and then diluted by a factor of 100 into fresh media and antibiotics. The total cell density as well as relative proportions of AmpR and ChlR cells are measured after 24 hours of growth, before the dilution step. **C)** Isolated co-cultures exhibit period 3 oscillations in the density of AmpR and ChlR cells (left panel) as well as in the ratio of AmpR cells to ChlR cells (right panel) under benign conditions. This experimental condition corresponds to 10 μg/ml of ampicillin and 8 μg/ml of chloramphenicol.

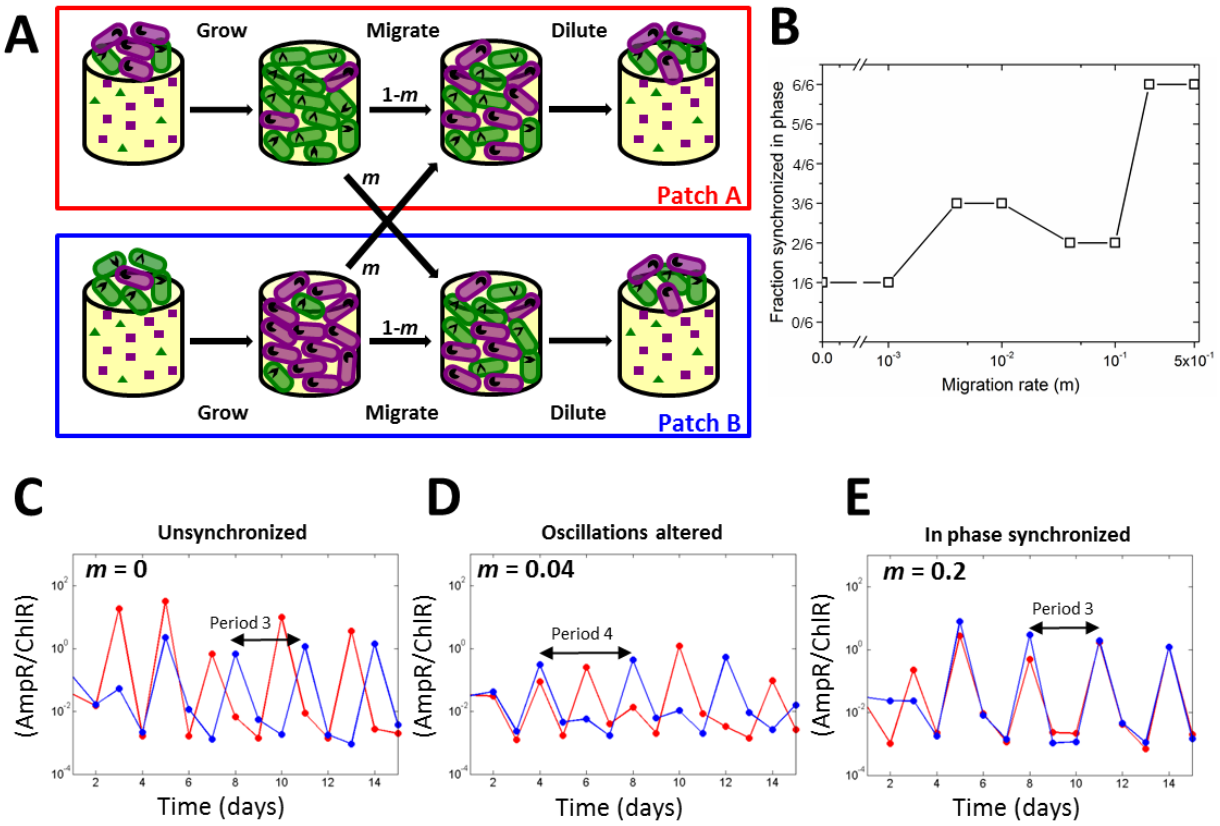

Fig 3: Increased migration rate leads to altered population dynamics and ultimately to synchronization. A) Schematic illustration of the growth-migration-dilution scheme employed in the experiments with two connected bacterial populations. The two patches A (red box) and B (blue box) correspond to two distinct co-cultures of AmpR and ChlR cells. The migration rate is denoted by *m*. **B)** The fraction (out of six replicates) of connected pairs of co-cultures synchronized in phase as a function of the migration rate in benign environmental conditions. **C-E)** Representative time series for the ratio of AmpR cells to ChlR cells in patches A (red plot) and B (blue plot) for $m = 0$ (**C**), $m = 0.04$ (**D**), and $m = 0.2$ (**E**), showing unsynchronized period 3 oscillations, disturbed oscillations with various periods and in-phase synchronized period 3 oscillations respectively. In **B-E**, the experimental condition corresponds to 10 μg/ml of ampicillin and 8 μg/ml of chloramphenicol.

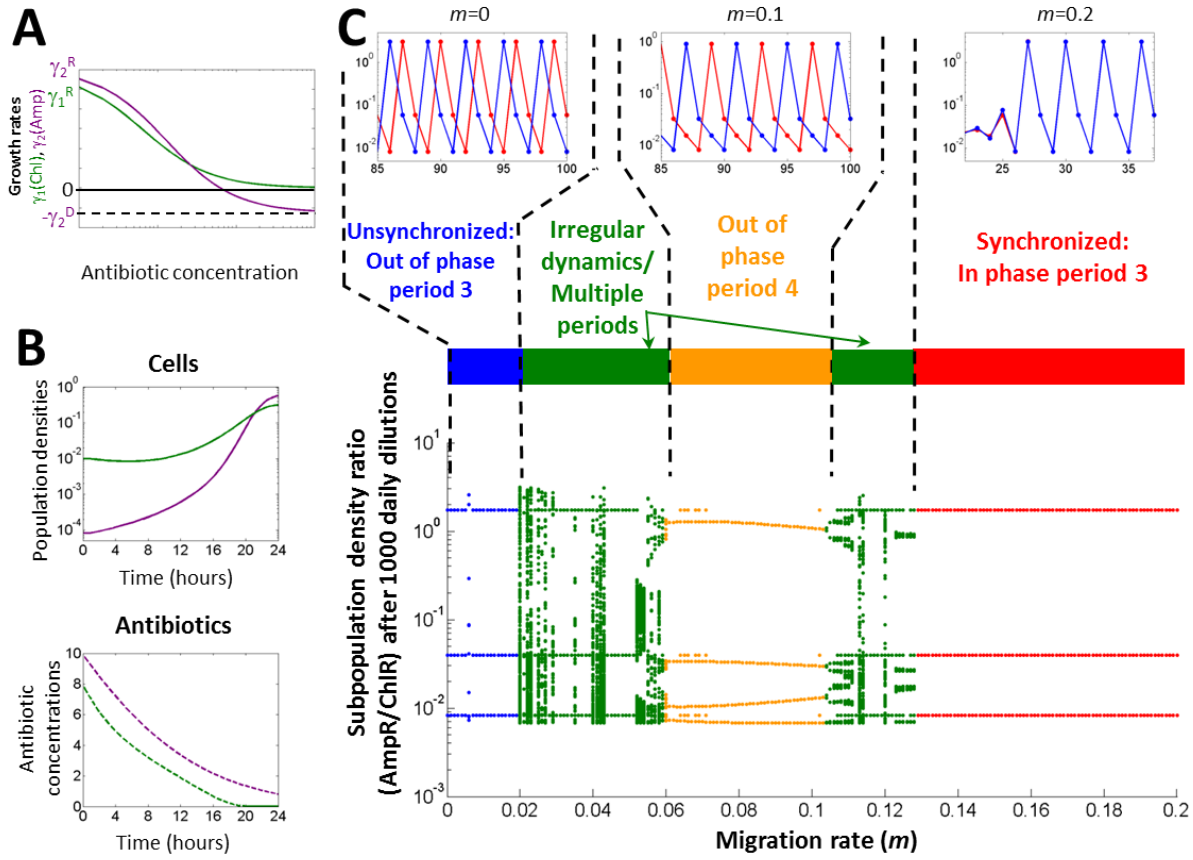

Fig 4: A mechanistic model of antibiotic degradation captures the experimentally observed sequence of dynamical outcomes. A) Dependence of growth rates on the concentration of antibiotics. **B)** Simulated ampicillin resistant (AmpR) and chloramphenicol resistant (ChlR) cell densities (top panel) and antibiotic concentrations (bottom panel) over the course of one 24 hour growth cycle, shown in purple and green respectively. **C)** Bifurcation diagram for a simulation of two co-cultures in a benign environmental condition (10 μg/ml of ampicillin, 8 μg/ml of chloramphenicol) as a function of the migration rate *m*. Unique values of the subpopulation density ratio (AmpR/ChlR) attained by patch A at the end of the growth cycle over the last 50 days of a simulation with 1000 daily dilutions are plotted for each migration rate. The simulations are deterministic. The diagram captures the sequence of observed dynamical outcomes: unsynchronized period 3 oscillations in the absence of migration, period-4 oscillations and irregular dynamics at intermediate migration rates, and in-phase synchronized period 3 oscillations at large migration rates. The insets in (C) show representative time series for $m = 0$, $m = 0.1$ and $m = 0.2$. Model parameters can be found in Table S1.

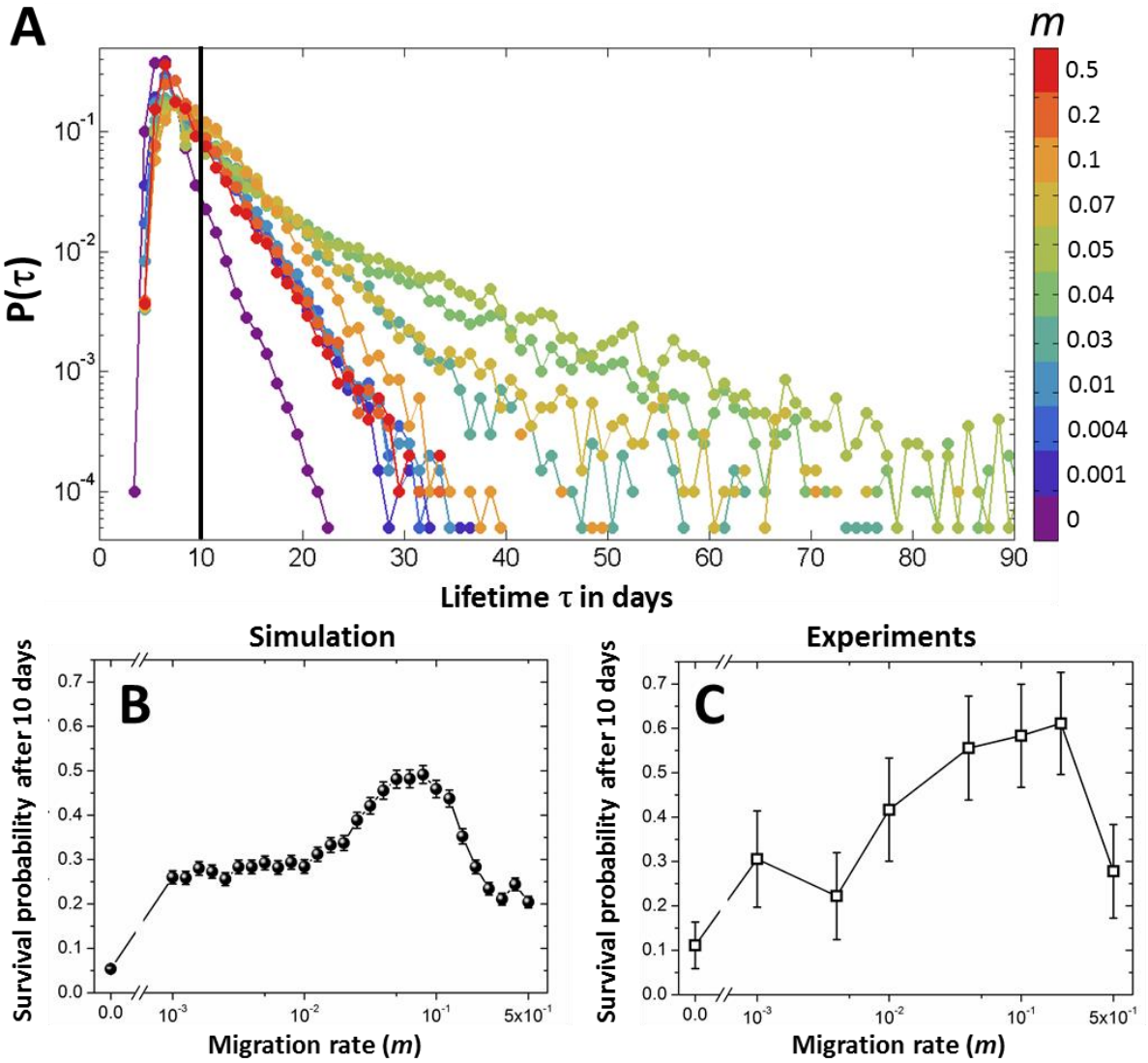

570

571 **Fig 5: Moderate levels of migration help populations survive longer in harsh environments.**
572 **A)** Simulated probability distributions of survival times of populations in a harsh environment (10
573 μg/ml of ampicillin, 16 μg/ml of chloramphenicol) for various migration rates. The distributions
574 were generated from 6000 simulation runs with initial conditions distributed around the three
575 phases of the period-3 oscillations observed in Fig. 4C. Connected patches were initialized in
576 different phases to avoid minimize synchronization. $P(\tau)$ is defined as the fraction of initial
577 conditions that survived for τ days. Different colors represent different migration rates, as
578 indicated in the colorbar. The survival time distributions have longer tails at intermediate migration
579 rates. The black vertical line indicates the threshold (10 days) used for calculating the survival

probability. This threshold was chosen to match the duration of the experiments. **B)** Simulated probability of survival after 10 days in the harsh environment as a function of the migration rate. **C)** Experimentally measured survival probability after 10 days as a function of the migration rate. Both (B) and (C) exhibit a maximum at intermediate migration rates, demonstrating that moderate amounts of migration help populations to survive longer in harsh environments. The error bars in (B) and (C) are standard errors of proportion.